Journal of Environmental Management 319 (2022) 115704



Contents lists available at ScienceDirect

Journal of Environmental Management

journal homepage: www.elsevier.com/locate/jenvman



Research article



Gas transfer model for a multistage vortex aerator: A novel oxygen transfer system for dissolved oxygen improvement

Sung Hyuk Park [a,*], Bill Batchelor [b], Arnab Ghosh [c]

[a] Department of ICT Integrated Safe Ocean Smart Cities Engineering, Dong-A University, 37 Nakdong-daero Saha-gu, Busan, 49315, Republic of Korea
[b] Zachry Department of Civil and Environmental Engineering, Texas A&M University, College Station, TX, 77843, United States
[c] Department of Civil Engineering, Dong-A University, 37 Nakdong-daero Saha-gu, Busan, 49315, Republic of Korea

ARTICLE INFO

Keywords:
Dissolved oxygen
Pure oxygen
Oxygen transfer
In-line mixer
Vortex flow
Multistage vortex aerator

ABSTRACT

A novel aerator for enhancing the oxygen transfer rate and efficiency, named multistage vortex aerator (MVA), was developed. It uses vortex flow in repeated stages to increase the gas-liquid interfacial area and to decrease the thickness of the stagnant layer at the interface between the two phases. The basic characteristics of oxygen transfer using this aerator were investigated using the American Society of Civil Engineers standard procedure. The MVA could rapidly transfer oxygen to water to a concentration higher than 40 mg/L in 60 min owing to the effect of high purity oxygen, additional pressure induced by water and gas, and vortex flow dynamics. A gas transfer model was developed for describing the non-steady state operation of the aerator. This model is based on the mass and molar balances of oxygen in gas and water. It could successfully simulate the DO change inside the aerator. This study can help better understand the oxygen transfer mechanism and evaluate the performance of the new aerator at the various temperatures, pressures, and gas compositions found in diverse environmental systems.

1. Introduction

An appropriate supply of oxygen is essential not only for humans, but also for aquatic environments. The decrease in oxygen concentration is a problem in both natural water and sewer systems. A low oxygen concentration in sewers results in anaerobic conditions, in which volatile fatty acids and hydrogen sulfide are produced, resulting in unpleasant odors (Huisman et al., 2004). High concentrations of hydrogen sulfide can even result in the death of sewer workers. Hence, cascades and chutes may be installed in sewer lines to increase the oxygen supply (Wójtowicz and Szlachta, 2016). Yuan et al. reported that 65% of the hydrogen sulfide generated in sewer pipes can be reduced by injecting 15–20 mg/L of oxygen into the pipes, and they suggested controlling the concentration of hydrogen sulfide in sewer lines through an optimized injection of oxygen (Ganigué and Yuan, 2014; Gutierrez et al., 2008; Jiang et al., 2015; Pikaar et al., 2014). The corrosion of concrete sewer pipes by sulfide has been reported to cost billions of dollars annually, and treating drinking water with 5.0–15.0 mg/L of sulfate-based coagulants resulted in a 30%–50% increase in the costs required to mitigate sewer corrosion. Furthermore, they concluded that more than 50% of the sulfate present in sewage originated from the aluminum sulfate coagulant used in the water treatment plant (Pikaar et al., 2014).

Oxygen injection is a popular technique for managing the water quality in rivers. The dissolved oxygen (DO) concentration of the Chicago waterway, one of the major tourist destinations in the United States, is maintained by using an aeration system (Alp and Melching, 2011). Campolo et al. investigated local oxygenation as an effective method to manage the water quality of the Arno river in Italy (Campolo et al., 2002). Several studies on managing reservoir water quality through aeration by destroying stratification and mixing the entire water body have been performed (Kim et al., 2006; Yum et al., 2008).

The removal of ammoniacal nitrogen (NH_4–N) from sewage is critical if water quality is to be preserved. Nitrification is typically used to remove ammonia from sewage. To ensure complete nitrification, a high level of dissolved oxygen (DO) (>2 mg/L) is recommended (How et al., 2018). Besides dissolved oxygen is key to avoiding odor and is critical for water quality improvement (Yoon et al., 2021; Boyd, 2015). Therefore, oxygen transfer is crucial in sewage treatment, and the air diffusing process in full-scale plants has been reported to account for 45%–70% of the total energy consumption (Rosso et al., 2008). Oxygen transfer methods include diffusing gas through a gas-liquid interface, releasing gas into a liquid through a semi-permeable membrane, and dissolving gas into a liquid using a novel device. The diffuser type, orifice size,

* Corresponding author.
E-mail address: shpark@dau.ac.kr (S.H. Park).

https://doi.org/10.1016/j.jenvman.2022.115704
Received 18 March 2022; Received in revised form 30 May 2022; Accepted 6 July 2022
Available online 14 July 2022
0301-4797/© 2022 The Authors. Published by Elsevier Ltd. This is an open access article under the CC BY-NC-ND license (http://creativecommons.org/licenses/by-nc-nd/4.0/).

Abbreviation

MVA	multistage vortex aerator
ASCE	American Society of Civil Engineers
K_La	overall oxygen transfer coefficient at the test temperature (1/min)
$K_La(20)$	overall oxygen transfer coefficient at 20 °C (1/min)
K_La_{MVA}	oxygen transfer coefficient for MVA (1/min)
C_{sat}	oxygen saturation concentration in water (mg/L)
SOTR	standard oxygen transfer rate (g/min)
SOTE	standard oxygen transfer efficiency (%)
DO	dissolved oxygen (mg/L)
V	volume of reactor (m^3)
Q_{O2}	volumetric oxygen supply rate (L/min)
F_{O2}	fraction of oxygen in gas (0.21 in air; 0.90 in oxygen gas)
V_i	volume of stage "i"
$C_{w,i}$	mass concentration of oxygen in water in stage "i"
T	time
Q_w	volumetric flow of water
R	Universal gas constant
$C_{s,i}$	mass saturation concentration of oxygen in water in stage "i"
θ_i	hydraulic retention time in stage "i", $\theta_i = V_i/Q_w$
V_t	volume of tank
$C_{w,t}$	mass concentration of oxygen in water in tank
$Q_{g,i}$	gas flow rate leaving stage "i"
$C_{g,I}$	mass concentration of oxygen in gas
$M_{t,i}$	molar concentration of gas at stage i, (mole/L), $M_{t,i} = P_i/RT$
$M_{t,0}$	total molar concentration in gas entering system, $M_{t,0} = P_0/RT$
$y_{o2,i}$	mole fraction of oxygen in gas in stage i
$y_{o2,0}$	mole fraction of oxygen in gas entering the aerator
$M_{o2,i}$	molar concentration of oxygen in gas, $M_{o2,i} = C_{g,i}/W_{o2}$
P_i	gas pressure in stage i (bar)
P_0	gas pressure applied to system (bar)
W_{o2}	molar mass of oxygen (32,000 mg/mol)
H	Henry's law constant
RFEP	relative fitting error parameter
SSR	sum of squared residuals

bubble size, submerged depth of the device, flow rates of air or oxygen, and device fouling are important factors (Demoyer et al., 2003; Garrido-Baserba et al., 2017; Gillot et al., 2005; Rosso et al., 2008; Rosso and Stenstrom, 2005; Zhou et al., 2013; Zhuang et al., 2016). Microporous diffusers release compressed air through small orifices, membrane pores, or other porous objects to create tiny bubbles. Fine bubble aeration has become the most widely used technique in sewage treatment because of its high energy efficiency (Fayolle et al., 2007; Rosso and Stenstrom, 2005). The oxygen transfer efficiency of these diffusers is proportional to the immersion depth, number of devices used, and surface area. In addition, the air flow rate affects the fluid dynamics of the bubbles. The higher the flow rate, the larger is the bubble, the smaller is the specific surface area, and the higher is the rising velocity of the bubble; these factors reduce the contact time between the gas and the liquid (Rosso and Stenstrom, 2005). Moreover, the oxygen transfer efficiency of a microbubble diffuser decreases with time, and the pressure required for backwashing gradually increases. This is due to the clogging of the pores of the diffuser or changes in the properties of the orifices of the polymeric membrane, which result in lower process efficiencies and higher power costs (Rosso and Stenstrom, 2006). Therefore, periodic cleaning of the devices used is required. In a recently published work Kim et al., (2021) reported that in waste-water treatment plants (WWTPs), conventional diffused aeration systems namely fine-bubble diffusers exhibit poor oxygen transfer, particularly when operating at high sludge concentrations.

Due to their susceptibility to diffuser fouling and ageing, the aeration efficiency of the fine pore diffusers decreases over time and also incurs high maintenance costs (Gillot et al., 2005; Rosso and Stenstrom, 2006; USEPA, U.S.E.P.A., 1989; Wagner and Popel, 1998). As a result, the amount of energy required to supply the same amount of oxygen to the biological process increases over time, eventually reducing its efficiency by 50% (Garrido-Baserba et al., 2017; Rosso and Stenstrom, 2006). Moreover, the microporous aeration exhibits a lower oxygen utilization rate at a relatively shallow water depth.

Other aeration devices include submerged turbines or jet diffusers, which use mechanical energy to shear large bubbles into fine bubbles to increase the gas-liquid interface area. Furthermore, the oxygen transfer in sewer pipes has been evaluated using a vortex flow regulator, which was used to quickly remove water for urban flood control (Wójtowicz and Szlachta, 2016).

In this study, we developed a novel system that uses an in-line mixer to maximize the oxygen transfer in various environmental processes. The developed aeration system rapidly transfers oxygen at higher efficiency and could be a promising alternative to conventional microbubble aeration. According to the two-film theory proposed by Lewis and Whitman in 1924, gas absorption depends on the thickness of a stagnant layer at the interface between a gas and a liquid, and any factor that can reduce the thickness of this layer increases the absorption rate (Lewis and Whitman, 1924). It is well documented the action of strong turbulence reduces the film thickness (Dai et al., 2020). As a result, the resistance to free surface mass transfer was reduced, which aided oxygen transfer. That is, such a process expedites the mass transfer rate at the free surface. Therefore vortex aeration which induces strong turbulence can be a promising alternative to microporous aeration for efficient oxygen transfer in water systems.

The primary mechanism of our system is a multistage vortex flow in a cylindrical structure. Once water is pumped with oxygen through separated inlets into the dissolver, the two phases collide in the cylindrical structure in the first stage and are mixed by a vortex flow that promotes oxygen transfer. Next, they proceed to the second stage, and this mechanism is repeated until the eleventh and final stage, with an increasing number of collisions occurring between the two phases as they progress through the stages. The vortex flow increases the interfacial area and decreases the thickness of the stagnant layer at the interface between water and oxygen, which results in an increased oxygen absorption rate. In this study, the basic oxygen transfer characteristics obtained using this new device were investigated, and a non-steady model was developed to simulate its performance.

2. Materials and methods

2.1. Multistage vortex aerator (MVA)

The oxygen dissolving device developed here is shown in Fig. 1. It has a liquid inlet and a gas inlet on the side of the cylindrical structure. Oxygen injected through the gas inlet collides with water and enters the cylinder. The inside of the cylinder comprises eleven stages connected by elbow pipes. Each elbow pipe was installed by rotating its inlet to an angle of 360/11° from the central axis. The gas and the liquid mixture, i.e., oxygen and water, occur using the vortex flow induced by the inner structure. By traversing all the stages of the device, water collides with oxygen, and when it exits the aerator, it has a high concentration of oxygen. The novel device developed in this study is called a multistage vortex aerator (MVA). In this device, diffusion, dispersion, and

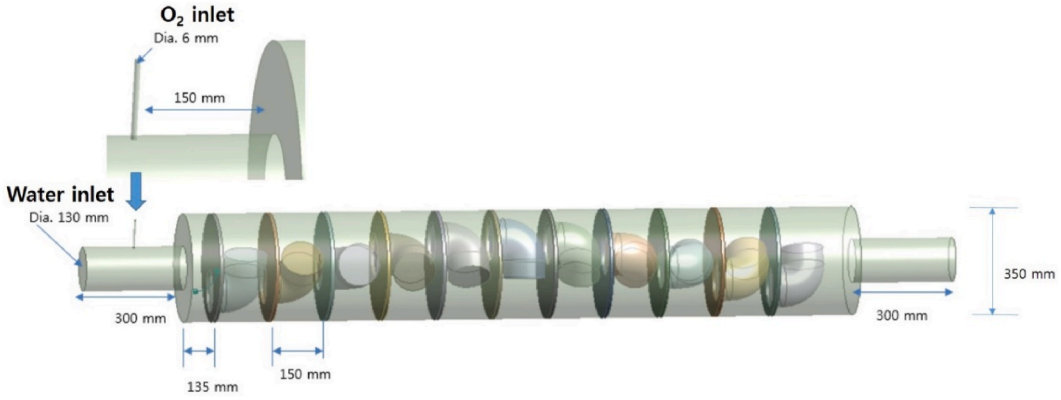


Fig. 1. Structure of multistage vortex aerator (MVA).

advection occur. Diffusion is a molecular Brownian motion that occurs in both laminar and turbulent flows; thus, it is the transport mechanism that carries oxygen through the stagnant layer in water at the gas-liquid interface. Transport through this layer typically controls the overall oxygen transfer rate and is proportional to the difference between the oxygen saturation concentration and the actual concentration of oxygen in the water. The saturation concentration is the concentration of oxygen that would exist in water if it were in equilibrium with the oxygen concentration in the gas. According to Henry's law, the saturation concentration of a gas dissolved in water is a function of the type of gas, the partial pressure of the gas in contact with water, and the total pressure applied. MVA can be used with high purity oxygen, ensuring that its higher partial pressure will increase the saturation concentration. Furthermore, additional pressure inside the cylinder will also increase the saturation concentration and, thereby, increase the oxygen transfer rate. Advection through the MVA induces turbulence, which increases the rate of oxygen transfer by reducing the thickness of the stagnant layer and increasing the gas-water interfacial area by reducing the bubble size.

The MVA can be considered as a plug flow reactor with dispersion, which occurs in three dimensions; additionally, it can be modeled as a set of completely mixed reactors in series. The multistage vortex aerator was manufactured by Deojon Korea Co., in Korea. Its diameter, length, and inner elbow diameter are 350, 2,300, and 100 mm, respectively. An oxygen generator (Oxus Co., Ltd, Korea) was used to produce a gas with a concentration of oxygen over 90%. For the comparison with the MVA, experiments were conducted with a ceramic-type air diffuser (Φ132 × 19H, Daeyang, Korea) and a bubble generator (HU07338-5017, KETI, Korea).

2.2. Basic oxygen transfer model

Theoretically, the kinetics of gas transfer is affected by the concentration gradient of dissolved oxygen in the stagnant layer in water adjacent to the gas-liquid interfaces through which diffusion occurs. The two-film theory is widely used to describe gas-liquid mass transport, and it is based on the physical model of double layers at the gas-liquid interface. It assumes that two stationary films exist at the interface between a gas and a liquid, and that the gas diffuses through the gas film in proportion to the existing concentration gradient across the film. Diffusion will not occur in the gas film if the gas is absolutely pure, since the concentration is constant throughout the gas film. Diffusion through the liquid film is controlled by the difference between the concentration values at the edges of the film. Since the liquid density is much greater than that of the gas, the resistance to diffusion is greater in the liquid (Lewis and Whitman, 1924); therefore, the transport through the liquid film usually controls the overall rate of oxygen transfer.

Hence, the oxygen absorption rate by water depends primarily on the oxygen concentration gradient across the liquid film at the gas-liquid interface. The concentration gradient is the difference between the oxygen concentration in the liquid film at the gas-liquid interface and the oxygen concentration in the liquid at the interface with the bulk liquid, divided by the thickness of the film. Since there is little resistance to oxygen transfer in the gas film, the concentration in the gas film at the gas-liquid interface will be nearly the same as that in the bulk gas. The model assumes that there is equilibrium between the gas and the liquid at the gas-liquid interface; therefore, the liquid film concentration there is equal to the saturated oxygen concentration C_{sat}, i.e., the concentration in water if it were in equilibrium with the concentration in the gas. These assumptions provide a basis for describing the rate of oxygen transfer that can be used in a mass balance of DO in a well-mixed volume of water (V) without inflow, outflow, or reactions producing or removing oxygen. This balance can be expressed as follows:

$$\frac{dC}{dt} = K_L \frac{A}{V}(C_{sat} - C) \tag{1}$$

where K_L is the overall mass transfer coefficient in the liquid phase, and A is the area through which oxygen is diffused. The term A/V is known as the specific interfacial area (a), which is difficult to measure. For practical purposes, the parameters K_L and A are typically combined to form $K_L a_{(T)}$, which represents the overall oxygen transfer coefficient at the test temperature.

After integration (for the initial condition $C = C_0$ at $t = 0$), Eq. (1) can be expressed in the exponential form:

$$\ln \frac{C_{sat} - C}{C_{sat} - C_0} = -K_L a_{(T)} \times t \tag{2}$$

Solving for C yields the following:

$$C = C_{sat} - (C_{sat} - C_0)\exp\left(-K_L a_{(T)} \times t\right) \tag{3}$$

The overall oxygen transfer coefficient values can be obtained by fitting the measured data to Eq. (2). The measured values can be adjusted to standard conditions (101.325 kPa, 20 °C) using an Arrhenius-type temperature correction in the following form:

$$K_L a_{(20)} = K_L a_{(T)} \times \theta^{(20-T)} \tag{4}$$

A typical value of exponential temperature coefficient $\theta = 1.0241$ was used.

The standard oxygen transfer rate (SOTR) is the instantaneous oxygen transfer rate that would be observed under standard conditions with no DO. It is not expressed per unit of volume and can be calculated as follows:

$$\text{SOTR} = K_L a_{(20)} \times C_{sat} \times V \tag{5}$$

where V is the volume of the reactor.

The standard oxygen transfer efficiency (SOTE) can be calculated as follows:

$$\text{SOTE}\ (\%) = \frac{\textit{Standard oxygen transfer rate}}{\textit{Oxygen supply rate}} \times 100 = \frac{SOTR}{Q_{O_2} \times 1.331 \times F_{O_2}} \times 100 \quad (6)$$

where Qo_2 is the volumetric oxygen supply rate (L/min), Fo_2 is the fraction of oxygen in gas (0.21 in air; 0.90 in oxygen gas), and 1.331 is the mass of oxygen per volume at 20 °C (g/L).

The experimental data for the dissolved oxygen concentration as a function of time were analyzed using nonlinear least-squares regressions to determine the values of K_La and C_{sat}. The values used for the modeled oxygen concentration at given values of K_La and Csat that were used in the regressions were obtained using the MATLAB function "nlinfit" to solve Eq. (1). The values of K_La and C_{sat} obtained were adjusted to standard conditions, and the SOTR (mass of oxygen dissolved per unit of time at a hypothetical DO concentration of zero) and SOTE were calculated.

2.3 Gas transfer model for the MVA

2.3.1 Model derivation

We developed a model that describes the non-steady state operation of the MVA. The model is based on the following assumptions: 1) there are eleven stages in the aerator; 2) water and gas are thoroughly mixed in all stages; 3) the water flow rate, K_La, the influent gas flow rate, and the influent gas composition are constant; 4) the perfect gas law applies; 5) gases other than oxygen do not transfer to water; and 6) oxygen does not undergo any reactions that would produce or destroy it.

1) Non-steady state material balance on oxygen in water in stage "i"

A non-steady state material balance on oxygen in water in stage "i" is:

$$\text{Accumulation} = \text{In} - \text{Out} + \text{Formed} - \text{Lost}$$

$$V_i\frac{dC_{w,i}}{dt} = Q_wC_{w,i-1} + V_iK_La_{MVA}\left(C_{s,i} - C_{w,i}\right) - Q_wC_{w,i}$$
$$\frac{dC_{w,i}}{dt} = \frac{C_{w,i-1} - C_{w,i}}{\theta_i} + K_La_{MVA}\left(C_{s,i} - C_{w,i}\right) \quad (7)$$

where V_i is the volume of stage "i," $C_{w,i}$ is the mass concentration of oxygen in water in stage "i," t is the time, Q_w is the volumetric flow of water, K_La_{MVA} is the oxygen transfer coefficient for the MVA, $C_{s,i}$ is the mass saturation concentration of oxygen in water in stage "i," and θ_i is the hydraulic retention time in stage "i" (V_i/Q_w).

2) Non-steady state balance on oxygen in water in tank

$$\text{Accumulation} = \text{In} - \text{Out} + \text{Formed} - \text{Lost}$$

$$V_t\frac{dC_{w,t}}{dt} = Q_wC_{w,11} - Q_wC_{w,t}$$
$$\frac{dC_{w,t}}{dt} = \frac{C_{w,11} - C_{w,t}}{\theta_t} \quad (8)$$

where V_t is the volume of the tank, and $C_{w,t}$ is the mass concentration of oxygen in water in the tank. Note that the input to the tank is the flow from the last stage of the aerator (i = 11).

3) Steady-state material balance on oxygen in both gas and water in stage "i"

We can assume a steady-state for this balance because the changes in the total amount of oxygen in water and gas do not change much with time after the first minute or so, when water at the initial oxygen concentration is flushed through the aerator. The model output shows that the rate of change in the total amount of oxygen (water and gas) in a stage is a small fraction of the total oxygen flow (water and gas) leaving and entering that same stage. This indicates that the rate of oxygen in the water and the gas entering stage "i" is the same as the rate of oxygen in the water and gas flowing out of stage "i." Therefore, we assume that the derivative of the amount of oxygen in the stage considering both air and water is zero.

A steady-state material balance on oxygen in both air and water in stage "i" is:

$$0 = \text{In} - \text{Out} + 0 - 0$$

$$0 = \left(Q_{g,i-1}C_{g,i-1} + Q_wC_{w,i-1}\right) - \left(Q_{g,i}C_{g,i} + Q_wC_{w,i}\right)$$
$$\left(Q_{g,i}C_{g,i} + Q_wC_{w,i}\right) = \left(Q_{g,i-1}C_{g,i-1} + Q_wC_{w,i-1}\right) \quad (9)$$

where $Q_{g,i}$ is the gas flow rate leaving stage "i," and $C_{g,i}$ is the mass concentration of oxygen in the gas.

4) Molar flow balance on oxygen in gas and water in stage "i"

The molar flow in the gas is the sum of the molar flow of oxygen and the molar flow of all other gases. The molar flow of all the other gases remains constant throughout the stages because the other gases are not transferred to water. Since 78% of air is nitrogen, the 90% purity oxygen gas produced from air is assumed to be composed of 90% oxygen and about 10% nitrogen gas. The unitless Henry's constants for oxygen and nitrogen are 30.75 and 60.16, respectively, meaning that nitrogen is more difficult to be transferred to water. Therefore, the molar flow of other gases (represented by nitrogen) in any stage is assumed to be equal to the molar flow of other gases entering the aerator.

$$\text{Total molar flow of gas} = \text{molar flow of oxygen} + \text{molar flow of other gases}$$

$$Q_{g,i}M_{t,i} = Q_{g,i}M_{t,i}y_{O2,i} + Q_{g,0}M_{t,0}\left(1 - y_{O2,0}\right)$$

where $M_{t,i}$ is the total molar concentration of gas at stage i, (mol/L), $M_{t,i} = P_i/RT$, $M_{t,0}$ is the total molar concentration in the gas entering the system ($M_{t,0} = P_0/RT$), $y_{O2,i}$ is the mole fraction of oxygen in the gas in stage i, and $y_{O2,0}$ is the mole fraction of oxygen in the gas entering the aerator.

$$Q_{g,i} = Q_{g,i}y_{O2,i} + Q_{g,0}\left(1 - y_{O2,0}\right)\frac{M_{t,0}}{M_{t,i}}$$

$$Q_{g,i} = Q_{g,i}y_{O2,i} + Q_{g,0}\left(1 - y_{O2,0}\right)\frac{P_0}{P_i}$$

$$y_{O2,i} = \frac{M_{O2,i}}{M_{t,i}}$$

where $M_{O2,i}$ is the molar concentration of oxygen in gas ($M_{O2,i} = C_{g,i}/W_{O2}$), Pi is the gas pressure in stage i (kPa), P_0 is the gas pressure applied to the system (kPa), and W_{O2} is the molar mass of oxygen (32,000 mg/mol).

Substituting for $M_{O2,i}$ and $M_{t,i}$:

$y_{O2,i} = (C_{g,i}/W_{O2})/(P_i/RT)$

$y_{O2,i} = (C_{g,i}/P_i)(RT/W_{O2})$

Similarly,

$y_{O2,0} = (C_{g,0}/P_0)(RT/W_{O2})$

Substituting,

$$Q_{g,i} = Q_{g,i}\left(\frac{C_{g,i}}{P_i}\right)\left(\frac{RT}{W_{o2}}\right) + Q_{g,0}\left[1 - \left(\frac{C_{g,0}}{P_0}\right)\left(\frac{RT}{W_{o2}}\right)\right]\left(\frac{P_0}{P_1}\right)$$

Rearranging,

$$C_{g,i} = \frac{P_i W_{o2}}{RT} - \frac{Q_{g,0}}{Q_{g,i}}\left(\frac{P_0 W_{o2}}{RT} - C_{g,0}\right) \quad (10)$$

5) Apply Henry's Law for oxygen solubility:

$$C_{s,i} = \mathrm{H} y_{O2,i} P_i$$

The values of H can be calculated from tabular values of $C_{s,i}$ for air ($y_{O2,i} = 0.21$) at the temperature and pressure of the aerator.

Substituting for $y_{O2,i}$ in terms of $C_{g,i}$:

$$C_{s,i} = H\left[\frac{\left(\frac{C_{g,i}}{W_{o2}}\right)}{\left(\frac{P_i}{RT}\right)}\right] P_i \quad (11)$$

$$C_{s,i} = HC_{g,i}\left[\frac{RT}{W_{o2}}\right]$$

Furthermore, the numerical solution method of the ODEs for the aerator Eq. (7) and the tank Eq. (8), is discussed in the Appendix.

2.4. Experiments

Herein, we investigated whether a general diffuser or the newly developed aerator was more effective for the oxygen transfer purpose. First, 1000 L of anoxic water samples were prepared by injecting nitrogen gas into tap water in a cylindrical water tank with dimensions of 1.2 × 1.03 m (H × D). In the experiments, 90% pure oxygen, which was generated using an oxygen generator, was supplied at flow rates of 1, 2, and 3 L/min. The experimental conditions are shown in Table 1. After degassing the sample, oxygen was delivered using the MVA or the diffuser, and the DO concentration was measured using a DO meter (Oxy guard, Denmark). Water was circulated at a flow rate of 200 L/min, as shown in Fig. 2. Experiments were conducted at approximately 19.9–26.4 °C, and the pressures measured at the inlet and outlet of the MVA were 150 and 100 kPa, respectively.

3. Results and discussion

3.1. Oxygen transfer experiments

To evaluate the change in DO using a MVA and a conventional diffuser, experiments were conducted according to the conditions shown in Table 1. In the text below, "oxygen" means 90% purity oxygen.

Fig. 3 compares oxygen concentrations using the MVA with that using a diffuser. When 1, 2, and 3 L/min of oxygen were supplied to the MVA, the oxygen concentration in a tank reached 20.2, 31.8, and 40.3 mg/L after 60 min of operation. As the oxygen flow rate increased, the dissolved oxygen concentration increased. When oxygen was injected at the same flow rate to the MVA and to the diffuser, the DO concentration at 60 min was 2.3 times higher in the MVA at the oxygen flow rate of 1.0 L/min, 3.5 times higher at 2.0 L/min, and 2.0 times higher at 3.0 L/min. This difference occurred because a vortex flow formed inside the cylinder of the MVA over eleven stages, causing the repeated collision of oxygen and water. Moreover, increased pressure in the MVA had a great influence on oxygen dissolution. The pressure at the inlet of the aerator was 150 kPa, which affected the solubility of the gas. According to Henry's law, the saturation concentration of oxygen at 150 kPa is 1.5 times higher than that at 100 kPa. In a recent work, Kim et al. reported the oxygen transfer performance of a supersaturated oxygen aeration system (SDOX) (Kim et al., 2020, 2021). Although the dissolved oxygen concentration reached up to 350 mg/L, the system was operated at high pressure (800 kPa) conditions. Our MVA system offers the advantage of high oxygen transfer efficiency with a dissolved oxygen concentration of 40 mg/L at 150 kPa pressure. In addition, it is noteworthy to mention here that a high-pressure requires more energy consumption and ultimately contributes to a higher process economy. Therefore, we have examined the performance of our MVA at a pressure close to atmospheric pressure (101 kPa) so as to minimize the energy demand.

Table 1
Experimental conditions.

Conditions	MVA (90% O_2 supply)			Diffuser (90% O_2 supply)		
Gas flow rate (L/min)	1	2	3	1	2	3
Water circulation flow rate (L/min)	200 L/min				-	
Temperature (°C)	19.9	22.4	23.9	22.2	25.2	26.4

A nonlinear regression was used to calculate the K_La and C_{sat} values that best fit the experimental data, and these values were adjusted to 20 °C. It should be noted that the ASCE (American Society of Civil Engineers) standard for calculating the oxygen transfer parameters is intended to be applied to various surface aerators and subsurface oxygenation devices, including diffused air, static tubes, submerged turbines, and jet aerators (ASCE, 2006). The vortex aerator can hardly be assigned to any of these categories. Furthermore, almost all of the oxygen transfer occurs inside the aerator and not in the tank. Thus, the K_La and C_{sat} values calculated using the ASCE standard do not represent the mechanisms occurring in the MVA. For example, the K_La is equal to the rate of oxygen transfer per unit volume of the tank, divided by the driving force in the tank (C_{sat} – C). However, no oxygen is transferred from the gas to the liquid in the tank; instead, it is all transferred in the aerator, as shown in Fig. 2. We thought it might be useful to calculate the K_La and C_{sat} values using the standard ASCE procedure for comparison with other aeration systems, but the coefficients used for the vortex aerator in Table 2 should be regarded as apparent transfer and saturation coefficients. An oxygen transfer model that is fundamentally sound for the MVA will be presented later. The values of $K_La_{,20}$, $C_{sat,20}$, SOTR, and SOTE for the two systems are summarized in Table 2 with the 95% confidence intervals and are shown in Fig. 4a–c.

Fig. 4a shows that the vortex aerator increased the oxygen transfer coefficient as the oxygen flow rate increased. It was observed that the values of $K_La_{,20}$ were 1.04–2.5 times higher when using the MVA under all oxygen flow rates tested. $K_La_{,20}$ increases with an increased gas-liquid interfacial area, and higher gas flow rates typically result in higher surface areas. In previous studies, Lee et al. applied a microbubble air diffuser to a 12-m-high tower and obtained a K_La value of 0.391 min^{-1} (Lee et al., 2012); furthermore, Choi et al. obtained a value of 0.326 min^{-1} using a variable control aeration device (Cho et al., 2017). Their K_La values are about one order of magnitude higher than the maximum value obtained using the MVA, but it is noteworthy that a 12-m-high reactor was used in their study to increase the efficiency of oxygen delivery. This means that additional pressure and structure are needed to increase this coefficient.

The effect of the oxygen flow rate on SOTR is shown in Fig. 4b. These results show that the values of SOTR were 2.6–3.3 times higher when using the vortex aerator under all oxygen flow rates tested. As the flow rate of oxygen increased, the SOTR increased. The SOTE represents the rate of oxygen transferred to the water relative to the rate of oxygen applied to the system in the gas and is expressed as a percentage. Fig. 4c shows the effect of gas flow rate on SOTE in both systems. The standard oxygen transfer efficiency for the diffuser was between 14.1% and 18.7%, whereas it was between 45.3% and 59.2% for the MVA. Lee et al. reported that the SOTE could increase up to 72% in the 12-m-tall aeration tower (Lee et al., 2012). It is known that the SOTE can increase with the height or depth of the reactor, and that is why the SOTE per unit of depth (%/m) is often reported for diffused aeration systems. When diffusers are used for oxygen delivery, the higher the gas flow rate, the larger the bubble size and the larger the total bubble volume. The net result is typically an increase in the total interfacial area, resulting in an increase in K_La. However, the increase is lower than the proportional

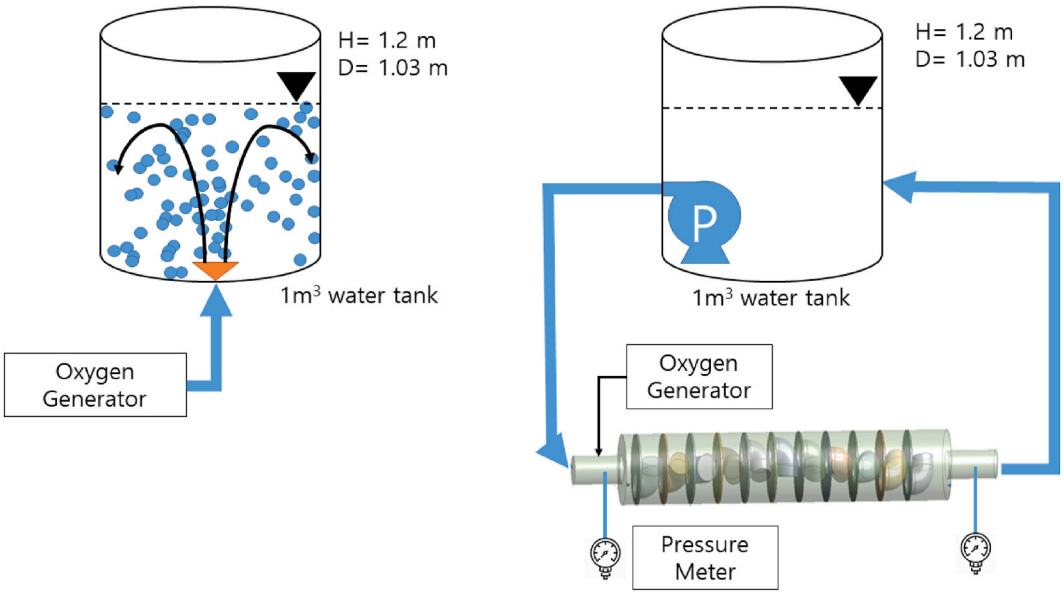


Fig. 2. Experimental configurations for oxygen transfer experiments.

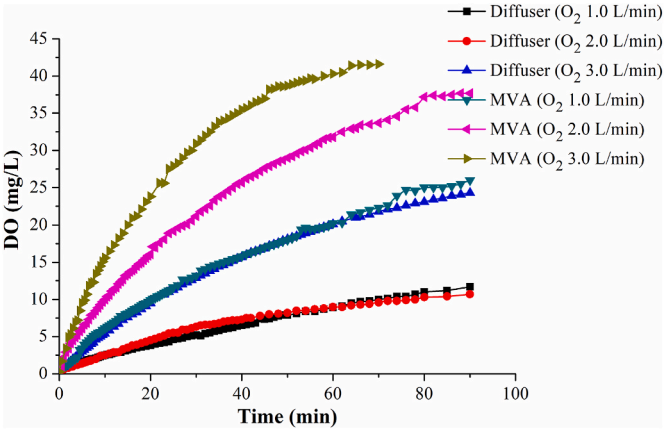


Fig. 3. Dissolved oxygen concentration over time using air diffuser and MVA.

Table 2
Values of $K_La_{,20}$, $C_{sat,20}$, SOTR, and SOTE for all experimental conditions.

	Vortex aerator			Diffuser		
	O_2 1.0 L/min	O_2 2.0 L/min	O_2 3.0 L/min	O_2 1.0 L/min	O_2 2.0 L/min	O_2 3.0 L/min
$K_La_{,20}$ ± 95% C.I.[a] (1/min)	0.016 ± 4.3%	0.026 ± 3.3%	0.045 ± 3.7%	0.011 ± 4.9%	0.025 ± 3.7%	0.018 ± 5.1%
$C_{sat,20}$ ± 95% C.I. (mg/L)	33.2 ± 2.3%	43.4 ± 1.7%	47.8 ± 1.7%	19.6 ± 2.9%	13.7 ± 1.9%	36.9 ± 3.0%
SOTR (g/min)	0.54	1.12	2.13	0.21	0.34	0.67
SOTE (%)	45.3	46.6	59.2	17.7	14.1	18.7

[a] The values with the confidence intervals were calculated using nonlinear regression; the values without confidence intervals were estimated using Eqs. (5) and (6). All values are adjusted to 20 °C.

increase in gas flow; therefore, the SOTE value typically decreases with the gas flow rate (Demoyer et al., 2003; Gillot et al., 2005; Kim et al., 2010; Yum et al., 2008; Zhou et al., 2013; Zhuang et al., 2016). However, the opposite phenomenon occurred in the vortex aerator. As the flow rate increased from 1 to 3 L/min, the SOTE also increased from 45.3% to 59.2% as depicted in Table 2. This shows that as the supplied gas flow increases, the SOTE increases faster than the proportional increase in the gas flow rate through repeated vortex flows. The increase in SOTE with an increase in flow rate is attributed to the mixing contribution due to the repeated collisions and turbulence generated in MVA from increasing the flow rate that aids in increasing the mass transfer between the air and the water. The resultant increase in SOTE reflects the effectiveness of the aeration process.

The multistage vortex aerator (MVA) can be a promising alternative to conventional aeration processes and can be explored in urban stream restoration and water quality improvement. In addition, the MVA can be applied in the stabilization of landfills, lagoons and sewage networks. The MVA supports high concentration oxygen injection into the sites and facilitates the quick conversion from an anaerobic to aerobic state, thereby preventing odor problems and enhancing water qualities.

3.2. Nonlinear regression and fitting of the proposed model

The oxygen transfer coefficient K_La for the MVA was obtained using least-squared, nonlinear regression of experimental data using MATLAB function "nlinfit". Fig. 4d shows how the proposed model was fitted to the experimental data. In Table 3, the K_La_{MVA} values vary from 0.075 to 0.41 min^{-1}, being 4.7 to 8.4 times greater than those calculated using the ASCE standard model. However, it is unreasonable to compare those values directly because they were obtained using different models.

In the case of flow rates of 2.0 and 3.0 L/min, the experimental results and the model showed similar trends. In the case of a flow rate of 1.0 L/min, the model predicted slightly lower K_La_{MVA} values than those obtained experimentally before the 60 min time point, and it predicted slightly higher values after 60 min. A relative fitting error parameter (RFEP) was calculated using the standard deviation of the data points relative to the regression line divided by the average value of the data. Therefore, it represents the ratio of the average error to the average value. The error parameter was helpful in determining the relative precision of fit. The RFEP values for probe data were calculated to be less than 0.1 (Table 3). Lower values represent better fits (lower errors) of the model to the data.

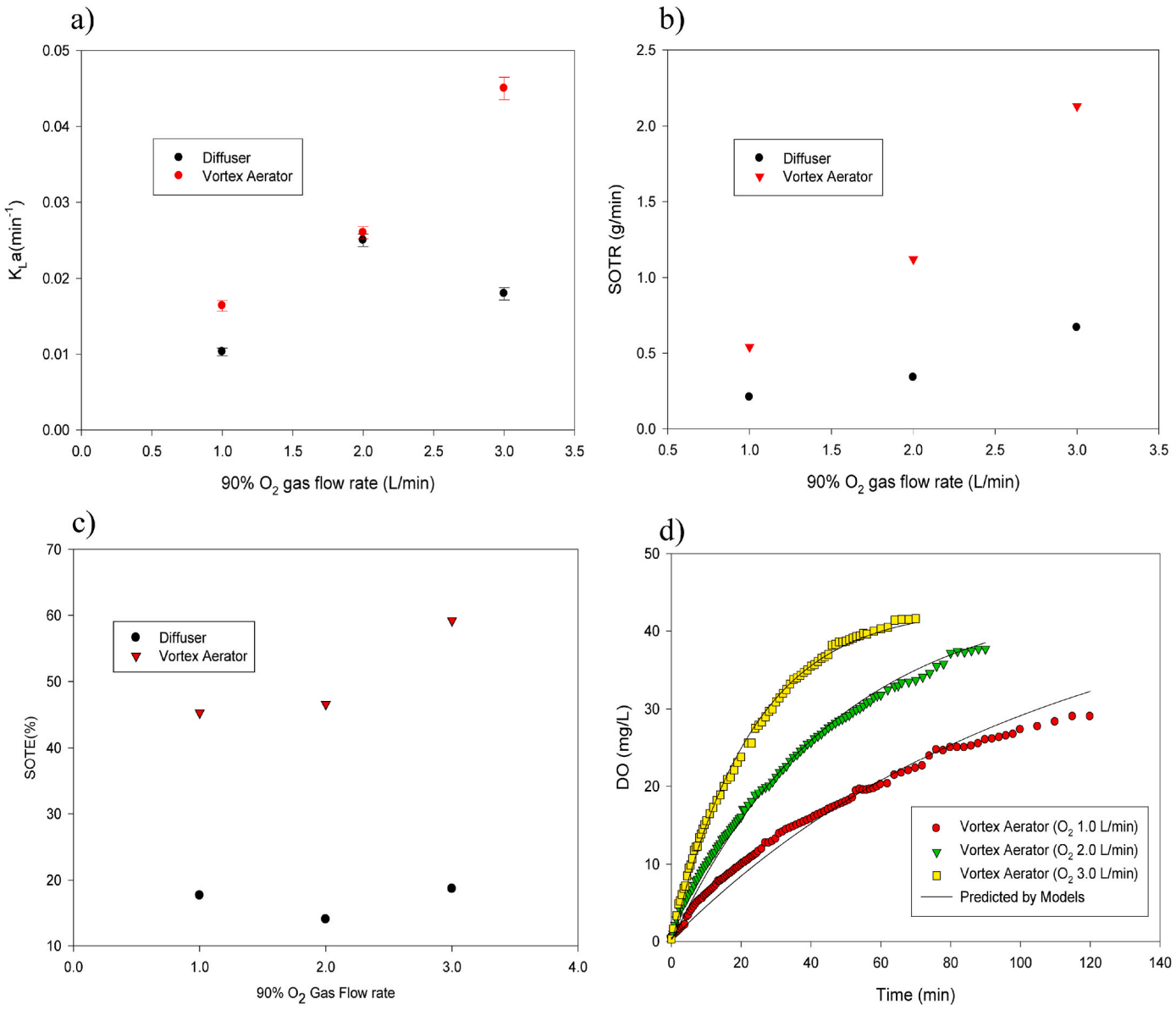


Fig. 4. a) Overall mass transfer coefficients as affected by O_2 flow rates at 20 °C calculated by ASCE standard model and New model for the multistage vortex aerator (MVA), b) Standard oxygen transfer rate at different O_2 flow rates c) Standard oxygen transfer efficiencies at different O_2 flow rates, d) Fitting of experimental data. The solid line represents model predictions.

Table 3
Oxygen transfer coefficients for MVA.

	O_2 1.0 L/min	O_2 2.0 L/min	O_2 3.0 L/min
K_La_{MVA} ± 95% C.I.[a] (1/min)	0.075 ± 2.3%	0.18 ± 1.6%	0.41 ± 1.9%
SSR[b] $(mg/L)^2$	167.2	79.5	41.4
RFEP[c]	0.090	0.045	0.030

[a] The values with confidence intervals were calculated using nonlinear regression.
[b] The Sum of Squared Residuals between the measured and calculated values of the concentration of oxygen.
[c] Relative fitting error parameter. All values are adjusted to 20 °C.

$$RFEP = \frac{\sqrt{\frac{SSR}{n-2}}}{\overline{C}}$$

where SSR is the Sum of Squared Residuals; n is the number of data points; and $\overline{C}$ is the average DO concentration.

3.3. Prediction using the proposed model

Fig. 5 (a), (b), and (c) show how the concentration of DO changes in the different stages of the aerator and in the tank over time, as predicted by the model. In Fig. 5 (a), the initial DO was 0.3 mg/L in all stages, and after 0.5 min, the DO increased to 1.9 mg/L in stage 1 and to 7.1 mg/L in stage 11. After 24 min, the first stage DO was 28.4 mg/L, and the last stage DO was 31.2 mg/L, and after 70 min, it was higher than 41 mg/L in all stages. The aerator seemed to be approaching the equilibrium state. In Fig. 5 (a), the C_{sat} values are represented at the top of the graph, being 51.6 mg/L in the first stage and 35.5 mg/L in the last stage at 70 min. Because of a higher pressure in the first stage, the saturation

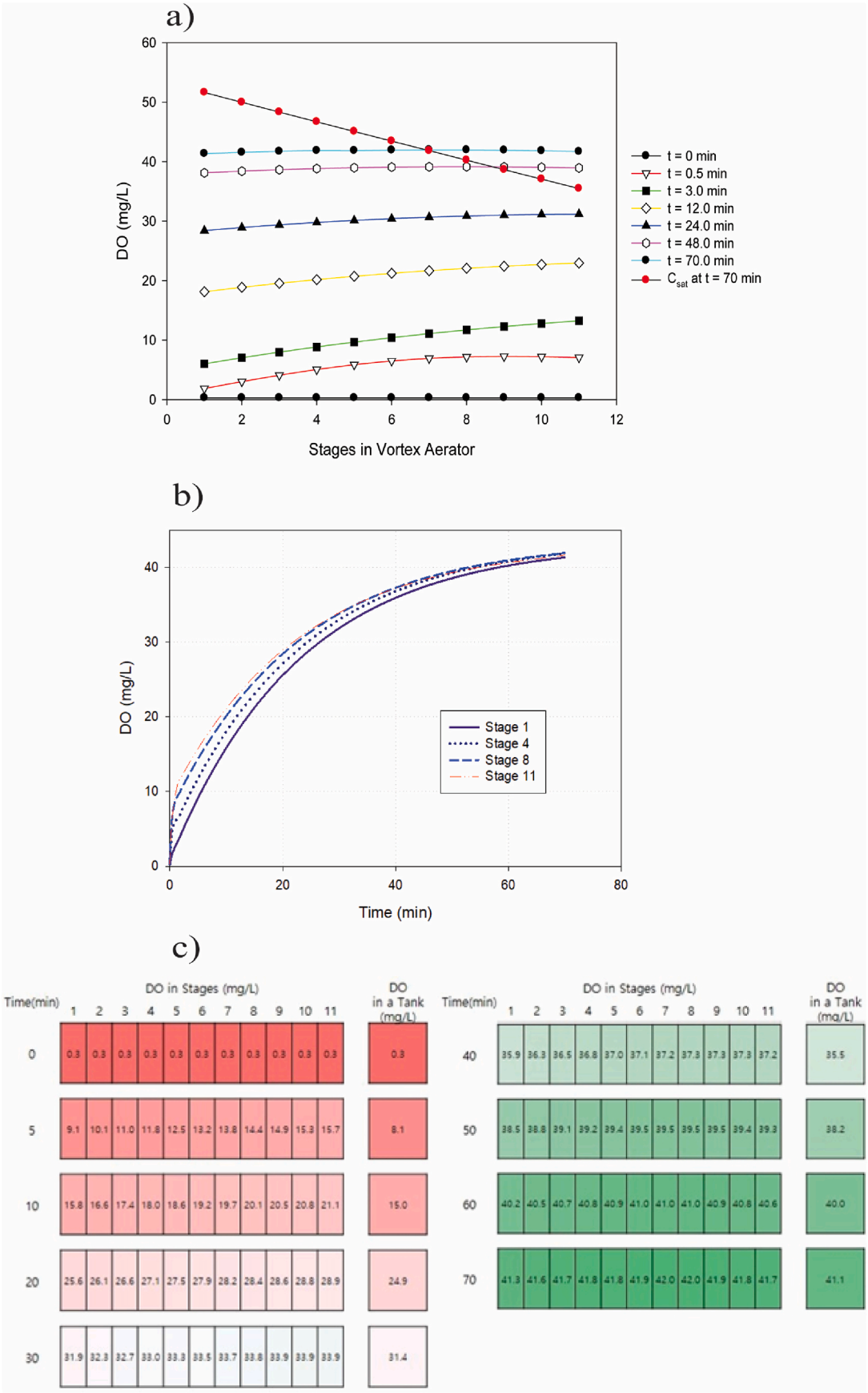


Fig. 5. Predicted dissolved oxygen (DO) profiles in multistage vortex aerator (MVA) and in Tank. (a) Predicted DO concentrations at each stages in MVA ($Qo_2 = 3.0$ L/min, $Q_w = 200$ L/min, T = 24 °C). (b) Predicted DO concentrations in MVA at different times ($Q_{O2} = 3.0$ L/min, $Q_w = 200$ L/min, T = 24 °C). (c) Predicted DO concentrations at each stages in MVA and in Tank.

concentration of oxygen is higher, and it decreases with the pressure drop at higher stages. Fig. 5 (b), illustrates the change in DO concentration with increasing time at different stages of the MVA. A high DO concentration in stage 11 relative to stage 1 suggest a increase in oxygen absorption rate due to increasing number of collsions between the two phases while progressing through different stages. The DO in different stages of MVA and in the tank at different time intervals is represented in Fig. 5 (c). It was observed that the MVA enhances the oxygen tranfer as it is evident from an increment in DO concentration in the tank from 0.3 mg/L to 41.1 mg/L after a time interval of 70 min. Therefore, the findings demonstrates the efficacy of the novel MVA system in dissolved oxygen improvement.

Fig. 6a and (b) show the calculated values of DO using the proposed model. Fig. 6a shows that the DO can rise to more than 60 mg/L when the pressure is changed from 150 to 300 kPa at 24 °C, at an oxygen supply of 3.0 L/min, and a water circulation flow rate of 200 L/min. Fig. 6b shows that, under the same conditions and under a pressure of 150 kPa, the DO can increase to more than 70 mg/L when the temperature is decreased to 0 °C. Therefore, a K_La of 0.41 min^{-1}, corresponding to a Q_{O2} of 3.0 L/min, was used (Table 3). Using this model, we predicted the oxygen dissolving performance of the MVA under various conditions, and these results can be used to study the optimal design conditions.

4. Conclusions

A new type of gas transfer device, called MVA, that induces a vortex in a multistage cylindrical structure, mixes gas and liquid, and transfers the gas to the liquid via diffusion, dispersion, and advection, was developed. Experiments and modeling research investigated its performance as an alternative to a conventional diffuser. The MVA was able to rapidly transfer oxygen to water because of the effect of the high partial pressure induced by high purity oxygen, the additional internal pressure exerted by water and gas, the decrease in the thickness of the stagnant layer caused by a vortex flow, and the increase in the contact area.

A model describing the oxygen transfer mechanism in the MVA was developed and applied to the experimental data. Using mass balance equations based on the two-film theory, we could derive a mathematical model suitable for the system. Although this model can be applied to describe the performance of the device regarding the pressure, temperature, and gas composition ratio when dissolving oxygen using MVA, it has some limitations. The main limitations of this model are its assumptions: (a) the K_La is the same in all stages, (b) the pressure drops linearly, and (c) the temperature is constant. As Q_g changes, the holdup (volume of gas in each stage) also shifts. This means that the surface area of the gas to transfer oxygen is altered, changing the actual value of K_La; therefore, there is probably some error in assuming that it remains constant in all stages. However, we expect that our results can guide future experimental research to optimize the product design.

Funding

The Dong-A University research fund supported this work.

Credit author statement

Sunghyuk Park: Conceptulalization, Methodology, Software, Validation, Investigation, Writing – original draft, Writing – review & editing, Supervision, Project administration. **Bill Batchelor**: Conceptulalization, Software, Validation, Formal analysis, Investigation, Data curation. **Arnab Ghosh**: Writing – review & editing, Visualization.

Declaration of competing interest

The authors declare that they have no known competing financial interests or personal relationships that could have appeared to influence the work reported in this paper.

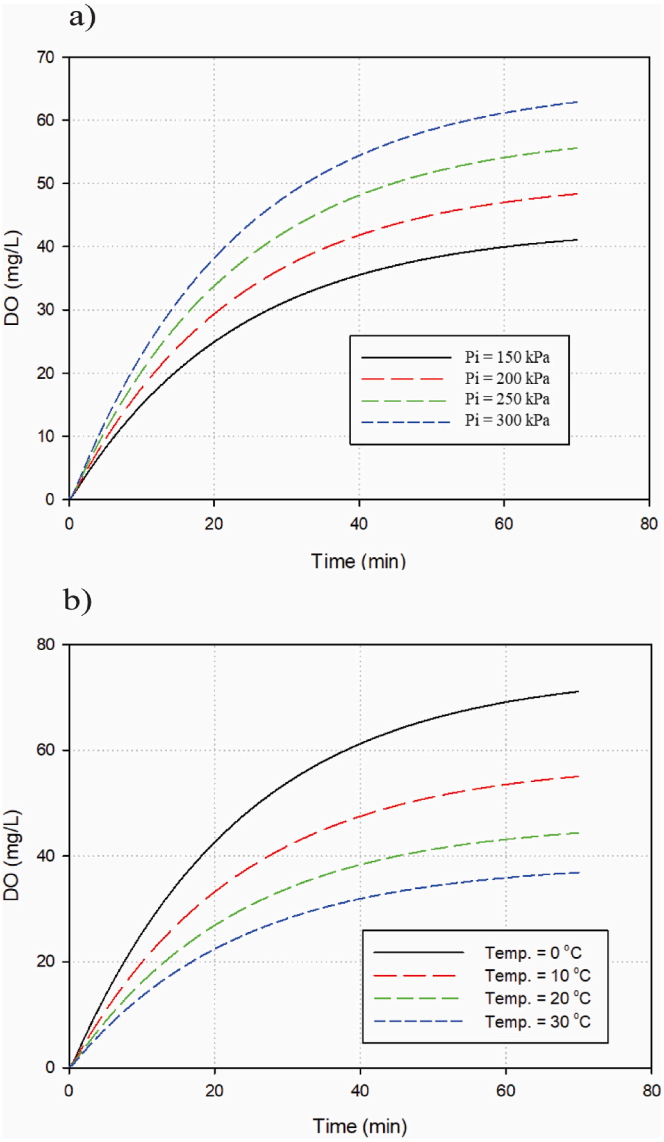


Fig. 6. Predicted dissolved oxygen (DO) profiles in multistage vortex aerator (MVA) at different a) pressure and b) temperature.

Appendix A. Supplementary data

Supplementary data to this article can be found online at https://doi.org/10.1016/j.jenvman.2022.115704.

References

American Society of Civil Engineers, 2006. Measurement of Oxygen Transfer in Clean Water. ASCE/EWRI 2-062006, Reston, Virginia.

Alp, E., Melching, C.S., 2011. Allocation of supplementary aeration stations in the Chicago waterway system for dissolved oxygen improvement. J. Environ. Manag. 92, 1577–1583. https://doi.org/10.1016/j.jenvman.2011.01.014.

Boyd, C.E., 2015. Dissolved oxygen and other gases. In: Water Quality. Springer, Cham. https://doi.org/10.1007/978-3-319-17446-4_6.

Campolo, M., Andreussi, P., Soldati, A., 2002. Water quality control in the river Arno. Water Res. 36, 2673–2680.

Cho, Y.J., Choi, Y.I., Jung, B.G., 2017. A study on the oxygen transfer characterization with a variable control aerator. J. Korean Soc. Environ. Eng. 18, 7.

Dai, C., Guo, J., Liu, J., Dong, L., Liu, H., 2020. Experimental study on aeration performance and bubble characteristics of inverted umbrella aerator. Water 12 (10), 2809. https://doi.org/10.3390/w12102809.

Demoyer, C.D., Schierholz, E.L., Gulliver, J.S., Wilhelms, S.C., 2003. Impact of bubble and free surface oxygen transfer on diffused aeration systems. Water Res. 37 8, 1890–1904.

Fayolle, Y., Cockx, A., Gillot, S., Roustan, M., Héduit, A., 2007. Oxygen transfer prediction in aeration tanks using CFD. Chem. Eng. Sci. 62, 7163–7171. https://doi.org/10.1016/j.ces.2007.08.082.

Ganigué, R., Yuan, Z., 2014. Impact of oxygen injection on CH_4 and N_2O emissions from rising main sewers. J. Environ. Manag. 144, 279–285. https://doi.org/10.1016/j.jenvman.2014.04.023.

Garrido-Baserba, M., Sobhani, R., Asvapathanagul, P., McCarthy, G.W., Olson, B.H., Odize, V., Al-Omari, A., Murthy, S., Nifong, A., Godwin, J., Bott, C.B., Stenstrom, M. K., Shaw, A.R., Rosso, D., 2017. Modelling the link amongst fine-pore diffuser fouling, oxygen transfer efficiency, and aeration energy intensity. Water Res. 111, 127–139. https://doi.org/10.1016/j.watres.2016.12.027.

Gillot, S., Capela-Marsal, S., Roustan, M., Héduit, A., 2005. Predicting oxygen transfer of fine bubble diffused aeration systems - model issued from dimensional analysis. Water Res. 39, 1379–1387. https://doi.org/10.1016/j.watres.2005.01.008.

Gutierrez, O., Mohanakrishnan, J., Sharma, K.R., Meyer, R.L., Keller, J., Yuan, Z., 2008. Evaluation of oxygen injection as a means of controlling sulfide production in a sewer system. Water Res. 42, 4549–4561. https://doi.org/10.1016/j.watres.2008.07.042.

How, S.W., Lim, S.Y., Lim, P.B., Aris, A.M., Ngoh, G.C., Curtis, T.P., Chua, A.S.M., 2018. Low-dissolved-oxygen nitrification in tropical sewage: an investigation on potential, performance and functional microbial community. Water Sci. Technol. 77 (9), 2274–2283. https://doi: 10.2166/wst.2018.143.

Huisman, J.L., Weber, N., Gujer, W., 2004. Reaeration in sewers. Water Res. 38, 1089–1100. https://doi.org/10.1016/j.watres.2003.11.025.

Jiang, G., Sun, J., Sharma, K.R., Yuan, Z., 2015. Corrosion and odor management in sewer systems. Curr. Opin. Biotechnol. 33, 192–197. https://doi.org/10.1016/j.copbio.2015.03.007.

Kim, J.Y., Park, S.H., Kim, S.H., Park, H., 2006. Laboratory-scale analysis of effect of plume spacing of air diffuser system on destrafication efficiency. Environ. Technol. 27, 1145–1152. https://doi.org/10.1080/09593332708618728.

Kim, S.H., Kim, J.-Y., Park, H., Park, N.-S., 2010. Effects of bubble size and diffusing area on destratification efficiency in bubble plumes of two-layer stratification. J. Hydraul. Eng. 136, 106. https://doi.org/10.1061/ASCEHY.1943-7900.0000152.

Kim, S.Y., Garcia, H.A., Lopez-Vazquez, C.M., Milligan, C., Herrera, A., Matosic, M., Curko, J., Brdjanovic, D., 2020. Oxygen transfer performance of a supersaturated oxygen aeration system (SDOX) evaluated at high biomass concentrations. Process Saf. Environ. Protect. 139, 171–181. https://doi.org/10.1016/j.psep.2020.03.026.

Kim, S.Y., Lopez-Vazquez, C.M., Curko, J., Matosic, M., Svetec, I.K., Štafa, A., Milligan, C., Herrera, A., Maestre, J.P., Kinney, K.A., Brdjanovic, D., Garcia, H.A., 2021. Supersaturated-oxygen aeration effects on a high-loaded membrane bioreactor (HL-MBR): biological performance and microbial population dynamics. Sci. Total Environ. 771, 144847 https://doi.org/10.1016/j.scitotenv.2020.144847.

Lee, S.J., Ko, K.H., Ko, M.H., Yang, J.K., Kim, Y.G., 2012. Oxygen transfer and hydraulic characteristics in bubble column bioreactor applied fine bubble air diffusing system. J. Korean Soc. Environ. Eng. 34, 8.

Lewis, K.W., Whitman, W.G., 1924. Principles of gas absorption. Ind. Eng. Chem. Res. 16, 1215.

Pikaar, I., Sharma, K.R., Hu, S., Gernjak, W., Keller, J., Yuan, Z., 2014. Reducing sewer corrosion through integrated urban water management. Science 345, 812–814. https://doi.org/10.1126/science.1251418.

Rosso, D., Larson, L.E., Stenstrom, M.K., 2008. Aeration of large-scale municipal wastewater treatment plants: state of the art. Water Sci. Technol. 57, 973–978. https://doi.org/10.2166/wst.2008.218.

Rosso, D., Stenstrom, M.K., 2006. Economic implications of fine-pore diffuser aging. Water Environ. Res. 78, 810–815. https://doi.org/10.2175/106143006x101683.

Rosso, D., Stenstrom, M.K., 2005. Comparative economic analysis of the impacts of mean cell retention time and denitrification on aeration systems. Water Res. 39, 3773–3780. https://doi.org/10.1016/j.watres.2005.07.002.

USEPA, U.S.E.P.A., 1989. Fine Pore (Fine Bubble) Aeration Systems.

Wagner, M.R., Popel, H.J., 1998. Oxygen transfer and aeration efficiency - influence of diffuser submergence, diffuser density, and blower type. Water Sci. Technol. 38, 1–6. https://doi:10.1016/S0273-1223(98)00445-4.

Wójtowicz, P., Szlachta, M., 2016. Experimental investigation and prediction of oxygen transfer in vortex flow regulators. Chem. Eng. J. 287, 337–349. https://doi.org/10.1016/j.cej.2015.11.035.

Yoon, D., Choi, M., Park, S., 2021. Urban streams' water quality and odor control using pure oxygen and vortex aerator. KSCE J. CEER. 41 (5), 493–504. https://doi.org/10.12652/Ksce.2021.41.5.0493.

Yum, K., Sung, H.K., Park, H., 2008. Effects of plume spacing and flowrate on destratification efficiency of air diffusers. Water Res. 42, 3249–3262. https://doi.org/10.1016/j.watres.2007.06.035.

Zhou, X., Wu, Y., Shi, H., Song, Y., 2013. Evaluation of oxygen transfer parameters of fine-bubble aeration system in plug flow aeration tank of wastewater treatment plant. J. Environ. Sci. 25, 295–301. https://doi.org/10.1016/S1001-0742(12)60062-X.

Zhuang, H., Hong, X., Han, H., Shan, S., 2016. Effect of pure oxygen fine bubbles on the organic matter removal and bacterial community evolution treating coal gasification wastewater by membrane bioreactor. Bioresour. Technol. 221, 262–269. https://doi.org/10.1016/j.biortech.2016.09.029.